JTTEE5 16:866–872
DOI: 10.1007/s11666-007-9092-x
1059-9630/$19.00 © ASM International

Peer Reviewed

HVOF-Sprayed Coatings Engineered from Mixtures of Nanostructured and Submicron Al_2O_3-TiO_2 Powders: An Enhanced Wear Performance

R.S. Lima, C. Moreau, and B.R. Marple

(Submitted February 27, 2007; in revised form August 8, 2007)

In previous studies, it has been demonstrated that nanostructured Al_2O_3-13 wt.%TiO_2 coatings deposited via air plasma spray (APS) exhibit higher wear resistance when compared to that of conventional coatings. This study aimed to verify if high-velocity oxy-fuel (HVOF)-sprayed Al_2O_3-13 wt.%TiO_2 coatings produced using hybrid (nano + submicron) powders could improve even further the already recognized good wear properties of the APS nanostructured coatings. According to the abrasion test results (ASTM G 64), there was an improvement in wear performance by a factor of 8 for the HVOF-sprayed hybrid coating as compared to the best performing APS conventional coating. When comparing both hybrid and conventional HVOF-sprayed coatings, there was an improvement in wear performance by a factor of 4 when using the hybrid material. The results show a significant antiwear improvement provided by the hybrid material. Scanning electron microscopy (SEM) at low/high magnifications showed the distinctive microstructure of the HVOF-sprayed hybrid coating, which helps to explain its excellent wear performance.

Keywords Al_2O_3-13 wt.%TiO_2, nanostructural characteristics, HVOF, in-flight particle characterization, microstructure, abrasion resistance

1. Introduction

1.1 Improved Wear Resistance of Air Plasma Sprayed Nanostructured Al_2O_3-13 wt.%TiO_2 Coatings

It has been demonstrated by other researchers that nanostructured Al_2O_3-13 wt.%TiO_2 coatings, made from nanostructured agglomerated powders and deposited via air plasma spray (APS), exhibit an enhanced wear performance when compared to conventional Al_2O_3-13 wt.%TiO_2 coatings (made from clad powders) also deposited via APS (Ref 1, 2). Surprisingly, it was observed that the nanostructured coatings were not harder than the conventional ones; however, the nanostructured coatings exhibited enhanced crack propagation resistance, i.e., they were tougher. This higher toughness of the nanostructured coatings is considered as the main characteristic responsible for their good wear performance levels.

1.2 Enhanced Wear Performance of HVOF-Sprayed Nanostructured Ceramic Oxide Coatings

In previous work, conventional (fused and crushed) and nanostructured TiO_2 powders were sprayed by APS and high-velocity oxy-fuel (HVOF). The abrasion wear of these coatings was tested. From the APS conventional to the HVOF-sprayed conventional TiO_2 coatings there was a reduction in the volume loss of 44%. However, from the APS conventional to the HVOF-sprayed nanostructured TiO_2 coatings there was a reduction in the volume loss of ~60% for the same wear testing conditions (Ref 3).

These results demonstrate that the wear performance of HVOF-sprayed nanostructured ceramics seems to be superior to that of APS conventional ceramics. Consequently, as Al_2O_3-13 wt.% TiO_2 is considered a more wear resistant material when compared to TiO_2, it is a logical step to apply the same concept to Al_2O_3-13 wt.% TiO_2.

2. Experimental Procedure

2.1 Powders

One nanostructured (as designated by the manufacturer) and two conventional Al_2O_3-13 wt.% TiO_2

This article is an invited paper selected from presentations at the 2007 International Thermal Spray Conference and has been expanded from the original presentation. It is simultaneously published in *Global Coating Solutions, Proceedings of the 2007 International Thermal Spray Conference*, Beijing, China, May 14-16, 2007, Basil R. Marple, Margaret M. Hyland, Yuk-Chiu Lau, Chang-Jiu Li, Rogerio S. Lima, and Ghislain Montavon, Ed., ASM International, Materials Park, OH, 2007.

R.S. Lima, C. Moreau, and **B.R. Marple**, National Research Council of Canada, 75 de Mortagne Blvd, Boucherville, QC, Canada J4B 6Y4. Contact e-mail: rogerio.lima@cnrc-nrc.gc.ca.

feedstock powders were employed in this work. The "nanostructured" Al_2O_3-13 wt.% TiO_2 feedstock (Nanox S2613S, Inframat Corp., Farmington, CT, USA) was made by spray-drying. This feedstock was sieved (air classifier) to separate the particles into two groups, fine cut for HVOF spraying and large cut for air plasma spraying. The first conventional feedstock Al_2O_3-13 wt.% TiO_2 (Metco 130, Sulzer Metco, Westbury, NY, USA) was made via the cladding of fused and crushed Al_2O_3 particles by a thin layer of submicron TiO_2 particles. The second Al_2O_3-13 wt.% TiO_2 feedstock (Amperit 744.0, H. C. Starck, Goslar, Germany) is a blend of Al_2O_3 and TiO_2 particles, and it was also sieved (air classifier) in order to obtain a fine particle cut for HVOF spraying. The particle size distribution of the powders was determined using a laser diffraction particle size analyzer (Beckman Coulter LS 13320, Beckman Coulter, Miami, FL, USA).

2.2 Torches and Thermal Spraying

The combination of powders, processes, and torches employed in this study can be found in Table 1. For the APS coatings (Ar/H_2 plasma), various spray parameters were initially tested by monitoring the particle temperature (T) and velocity (V) using a diagnostic tool based on pyrometric and time-of-flight measurements (DPV 2000, Tecnar Automation, Saint Bruno, QC, Canada). The parameter sets that produced a wide range of T & V values were selected for coating production. A total of three "nanostructured" and four conventional Al_2O_3-13 wt.% TiO_2 coatings were produced via APS. For HVOF spraying, various spray parameters were also initially tested by monitoring particle T & V by using the DPV 2000. The parameter set that produced the highest average particle temperature for the two feedstock powders was selected for coating production, i.e., two coatings (one "nanostructured" and one conventional) were produced via HVOF spraying. For each spraying case, a total of 5000 particles were measured at the centerline of the spray jet where the particle flow density was the highest. The particle detector was placed at the same spray distance as used when depositing the coatings.

The coatings were deposited on low-carbon steel substrates (width: 2.54 cm; length: 7.62 cm; thickness: 1.27 cm) that had been grit-blasted with alumina to roughen the surface before spraying. During the spraying process, a cooling system consisting of air jets was applied to reduce the coating temperature. The coating temperature was monitored during spraying using an optical pyrometer (focused at the coating surface). The maximum temperatures during the process were ~280 °C and ~180 °C, respectively, for the HVOF-sprayed and air plasma sprayed coatings. The typical coating thickness was 450-550 µm.

Table 1 Torches, processes and powders employed in this study

Powder	Process	Torch
Metco 130	APS	F4-MB*/SG100**
Nanox S2613S (APS cut)	APS	F4-MB*
Amperit 744.0 (HVOF cut)	HVOF	DJ2700-hybrid*
Nanox S2613S (HVOF cut)	HVOF	DJ2700-hybrid*

* Sulzer Metco, Westbury, NY, USA
** Praxair, Concord, NH, USA

2.3 Nanostructure, Microstructure, and Porosity

The nanostructural and microstructural features of the powders were analyzed via scanning electron microscopy (SEM). The overall coating microstructure and porosity were also analyzed via SEM and image analysis. A total of 10 images (500 X) per coating randomly located were analyzed to determine porosity levels.

2.4 Microhardness and Crack Propagation Resistance

Vickers microhardness measurements were performed under a 300 gf load for 15 s on the crosssections of the coatings. A total of 10 microhardness measurements were carried out for each coating. The crack propagation resistance was determined by indenting the coating crosssections with a Vickers indenter at a 5 kgf load for 15 s, with the indenter aligned such that one of its diagonals would be parallel to the substrate surface. The total length (tip-to-tip) of the major crack ($2c$) parallel to the substrate surface that originated at or near the corners of the Vickers indentation impression was measured. Based on the indentation load (P) and $2c$, the crack propagation resistance was calculated according to the relation between load and crack length $P/c^{3/2}$, where P is in Newtons and c is in meters (Ref 4). A total of five indentations were carried out for each coating. It is important to point out that the crack propagation resistance concept applied in this study is not an absolute measure of fracture toughness. To determine indentation fracture toughness, other parameters must be introduced in the calculation. However, crack propagation resistance data allows comparison of the different coatings and provides a basis for determining the relative effect of the thermal spray processing and powder morphology on crack propagation characteristics and wear performance.

2.5 Abrasion Wear Resistance

The abrasion resistance of the coatings was tested based on the standard ASTM G65-00 (procedure D, modified) (Ref 5), which is also known as the dry sand/rubber wheel test. In this test, a stationary-coated sample was pressed against a rotating rubber-coated wheel (diameter 228.6 mm; 200 rpm) with a force of 45 N. Silica sand (212-300 µm) was fed (300-400 g/min) between the coating and the rubber wheel until the wheel traveled over the equivalent linear distance of 1436 m. Prior to being tested, the surfaces of the coatings were prepared by grinding with diamond wheels to produce a leveled surface and a surface finish of $R_a \sim 0.2$ µm. Two samples were tested for each coating produced in this study. The volume of the material abraded away during the wear test was measured via optical profilometry.

Peer Reviewed

3. Results and Discussion

3.1 Feedstock Powders

The particle size cut of the powders is shown in Table 2. It can be observed that the powder particles employed for APS were larger than those employed for HVOF. It was previously shown that a particle-size distribution from 5 to 20 μm is approximately the optimal cut for HVOF spraying of ceramics (Ref 6). It is important to point out that the two groups of powders designated to be sprayed via HVOF and APS exhibited, in general, similar particle size cuts, respectively (Table 2). This characteristic is important in order to observe real effects of the feedstock structure (and not feedstock size) on the coating microstructure and properties. The SEM powder pictures can be found in Fig. 1 and 2. It is important to point out that these pictures (at low magnification) were taken using backscattered electrons (BSE). Therefore, differences in contrast can be related to differences in atomic numbers (e.g., Al: 13 and Ti: 22). The lower atomic number elements will appear darker than the heavier ones in the SEM picture. Figure 1 shows the SEM picture of the Al_2O_3-13 wt.% TiO_2 feedstock powder Amperit 744.0. It is possible to confirm that this feedstock is blended, i.e., formed by the mixture of fused and crushed Al_2O_3 and TiO_2 particles.

Figure 2 shows the "nanostructured" Al_2O_3-13 wt.% TiO_2 feedstock powder (Nanox S2613S). It is possible to confirm that this feedstock was formed by the agglomeration, via spray-drying, of individual Al_2O_3 and TiO_2 particles. Among the feedstock powders employed in this study, this one exhibits the highest degree of homogeneity (level of mixing of the Al_2O_3 and TiO_2 particles) (Fig. 2a). The particle of Fig. 2a, observed at higher SEM magnifications using secondary electrons (SE) is shown in Fig. 2b. It can be seen that the microscopic spray-dried material is formed by the agglomeration of individual particles with diameters varying from approximately 15 to 300 nm. Nanostructured material is normally defined as exhibiting grain/particle sizes that are less than 100 nm in at least one dimension, therefore this is not strictly a nanostructured feedstock. The expression "bimodal powder" or "hybrid powder," indicating the presence of nanostructured (i.e., <100 nm) and submicron particles (i.e., 100-500 nm), is more scientifically rigorous. Therefore, the term "hybrid powder" and "hybrid coating" will be used in this article to describe the Nanox S2613S Al_2O_3-13 wt.% TiO_2 feedstock powder and its coatings, respectively. Finally, it is important to point out that the hybrid particles are porous, which will probably influence the in-flight particle characteristics, as shown in the next section.

Table 2 Particle size distribution of the Al_2O_3-13 wt.% TiO_2 powders (in volume)

Powder	d_{10}, μm	d_{50}, μm	d_{90}, μm
Metco 130	24	36	53
Nanox S2613S (APS cut)	14	39	62
Amperit 744.0 (HVOF cut)	6	10	16
Nanox S2613S (HVOF cut)	2	15	24

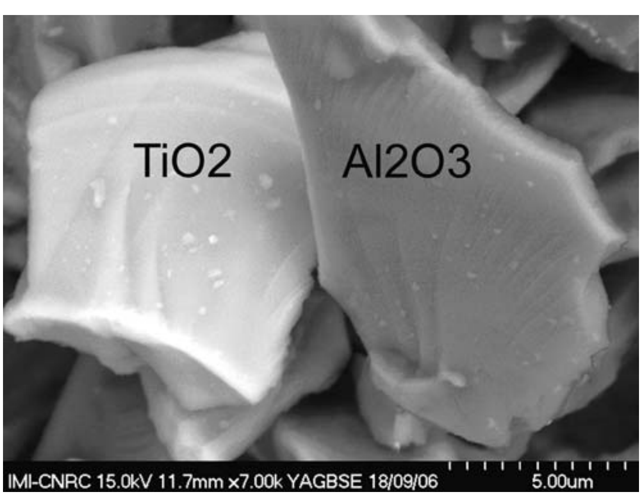

Fig. 1 SEM picture (BSE) of the Al_2O_3-13 wt.% TiO_2 powder Amperit 744.0

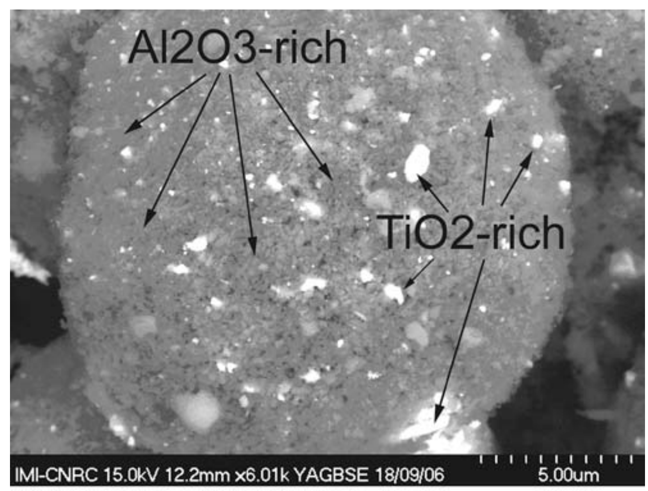

(a)

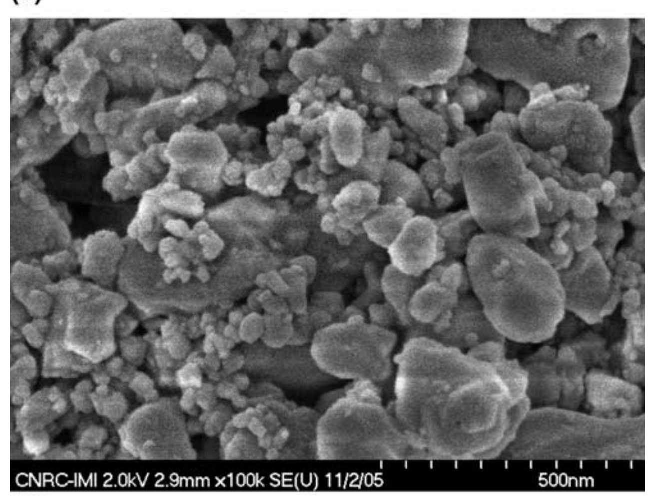

(b)

Fig. 2 (a) SEM picture (BSE) of the Al_2O_3-13 wt.% TiO_2 powder Nanox S2613S. (b) Particle of (a) observed at higher magnification (SE)

The second conventional Al_2O_3-13 wt.% TiO_2 feedstock powder (Metco 130) is clad, i.e., it was made via the cladding of fused and crushed Al_2O_3 particles by a thin layer of submicron TiO_2 particles. Detailed SEM pictures of this powder can be found in different references (Ref 1, 2).

3.2 In-Flight Particle Characteristics

The results of average T & V for the plasma sprayed powders were found to be in the range of (i) 2356-2700 °C and 261-367 m/s for the Metco 130 powder and (ii) 2479-2687 °C and 268-388 m/s for the Nanox S2613S (APS cut) powder, respectively. This wide range of average particle T & V resulted in a wide range of different coating microstructures being formed during thermal spraying, i.e., it may be stated that this is a fair representation of Al_2O_3-13 wt.% TiO_2 coatings that can be engineered via APS.

The average and standard deviation of the T & V for the HVOF-sprayed particle distributions were found to be (i) 2133 ± 138 °C and 863 ± 109 m/s for the Amperit 744.0 (HVOF cut) powder and (ii) 2382 ± 278 °C and 985 ± 95 m/s for the Nanox S2613S (HVOF cut) powder; therefore, the differences in particle temperature and velocity were not significant. The two types of HVOF-sprayed coatings were sprayed with the same set of spray parameters; however, the T & V values achieved by the hybrid powder were approximately 10% higher then those achieved by the conventional powder. It must be pointed out that the HVOF parameter set used to spray both powders corresponded to the maximum propylene flow that could be fed into the DJ2700-hybrid torch at a constant rate. Therefore, the difference of approximately 10% in T & V values between the two groups of feedstock particles was not intentionally produced. It is also important to point out that HVOF spraying of ceramic oxides is carried out at the limit of the HVOF systems, due to their low flame temperatures (typically below 3000 °C) and the high melting point of ceramic materials.

There is one hypothesis to explain this difference of T & V values observed when using the same spray parameters for both powders. The conventional particles are dense (Fig. 1), therefore, they should conduct heat better than the hybrid particles (Fig. 2), which are also porous. In addition, the hybrid particles have larger surface areas when compared to the conventional particles. Therefore, the large surface area probably translates into a better capacity to absorb heat from the HVOF flame. The porous structure of the hybrid powder could act as a thermal barrier, consequently the heat absorbed at the particle surface may propagate at lower rates toward the particle inner core when compared to those of the conventional fused and crushed fully dense particles. In addition, a hybrid particle of a given diameter would have a lower mass due to porosity; therefore, a given amount of heat transfer would produce a higher temperature than in a solid particle of the same diameter. As a general consequence, due to the higher surface area, lower mass, and lower thermal conductivity, the hybrid particles would have a tendency to exhibit higher surface temperatures, which are the temperatures measured by the pyrometric system of the DPV 2000. The higher particle velocities attained by the hybrid particles may be related to their lower densities (porous structure), i.e., they are lighter than the fully dense particles.

It is important to point out that this phenomenon of higher particle T & V values measured for the HVOF-sprayed hybrid particles was also observed during plasma spraying. When the same plasma spray parameters were used to spray the hybrid (Nanox S2613S) and conventional (Metco 130) powders, the T & V values measured for the hybrid powders were higher than those measured for the conventional (clad) powder. As the clad powder is fully dense, the same hypothesis can be used here to explain this difference of T & V values. However, as plasma spraying of ceramics does not have the same constraints of HVOF, higher plasma currents or H_2 flows (or both) were used for spraying the conventional feedstock (Metco 130) in order to attain T & V values similar to those measured for the hybrid particles.

3.3 Abrasion Wear Resistance

The abrasion wear resistance values of the coatings produced for this study were ranked in terms of volume loss, i.e., the lower the volume loss, the higher the wear resistance (Fig. 3). From Fig. 3 it is possible to observe that among the APS coatings, the four conventional ones exhibited lower wear resistance (i.e., higher volume loss) than the three hybrid coatings. However, the HVOF-sprayed conventional coating outperformed the best APS hybrid coating. Furthermore, the best performing anti-wear coating of all was the HVOF-sprayed hybrid coating. From the optimized ASP conventional coating to the HVOF-sprayed hybrid coating, there was a reduction in volume loss of 87%, or an improvement of eight times in wear performance.

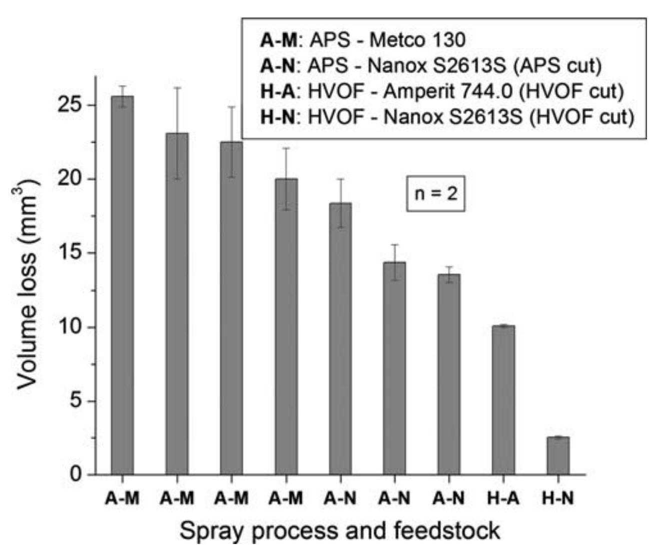

Fig. 3 Volume loss for each combination of spray process and feedstock

Peer Reviewed

The explanation for the enhanced wear behavior of APS coatings produced from spray-dried (nanostructured) Al_2O_3-13 wt.% TiO_2 powders when compared to conventional coatings (clad powder—Metco 130) has been hypothesized by different authors (Ref 1, 2). Gell et al. (Ref 1) hypothesized (with some level of experimental evidence) that semimolten nanostructured feedstock particles embedded in the coating microstructure would act as crack arresters, thereby increasing the toughness of the coatings. Ahn et al. (Ref 2) proposed another hypothesis (with some level of experimental evidence). The melting point of pure Al_2O_3 is ~2050 °C, whereas, the melting point of Al_2O_3-13 wt.% TiO_2 is ~1940 °C. Ahn et al. observed that the spray-dried nanoagglomerates exhibited a homogeneous mixing of Al_2O_3 and TiO_2 particles (such as that of Fig. 2), which in turn would tend to lower the melting point of each agglomerate (by the addition of TiO_2 to Al_2O_3), lowering particle viscosity, thereby improving the interlamellar contact (i.e., coating toughness) at impact during spraying (Ref 2). Due to the existence of these hypotheses for APS coatings, this work will concentrate on the development of a hypothesis for explaining the enhanced wear behavior of the HVOF-sprayed hybrid coatings, as shown in the next sections.

3.4 Hardness, Porosity, and Crack Propagation Resistance

Table 3 shows the porosity and Vickers microhardness values obtained for the coatings involved in this study. It is evident that the hardness values alone do not provide enough information to explain the enhanced wear performance of the HVOF-sprayed hybrid coating. For example, the crack propagation resistance values of the two HVOF-sprayed coatings were measured. The values were 30.5 ± 3.3 MPam ½ and 25.5 ± 0.7 MPam ½ for the hybrid (Nanox S2613S) and conventional coatings (Amperit 744.0), respectively. As a comparison, the Vickers microhardness (300 gf) and crack propagation resistance of the optimized APS Metco 130 (clad) coating were 1080 ± 58 and 14.0 ± 2.5 MPam ½, respectively. It can be deduced that the HVOF-sprayed hybrid coating was tougher than the conventional (blended) HVOF-sprayed and optimized conventional APS (clad) coatings. As previously stated in Section 2.4, it is important to point out that the crack propagation resistance is not an absolute measure of fracture toughness. However, these values are related to toughness and allow comparison of the different coatings and provide a basis for determining the relative effect of the thermal spray processing and powder morphology on crack propagation characteristics and wear performance.

This phenomenon was also observed by other authors, i.e., the superior wear resistance of these "nanostructured" ceramic thermal spray coatings (Fig. 3) cannot be explained based on simple average hardness values. The factor (property) that seems to be most important for the superior antiwear performance of these coatings is reported to be the crack propagation resistance or "relative toughness" (Ref 1, 2).

This difference in crack propagation resistance under Vickers indentation is shown in Fig. 4 and 5. From these pictures it is observed that the hybrid coating exhibits a more homogeneous microstructure than that of the conventional coating. Due to the nature of the conventional feedstock Amperit 744.0 (Fig. 1), it seems logical to assume that Al_2O_3 and TiO_2 particles will not be homogeneously mixed in the coating microstructure. Therefore the white-colored and dark-colored regions in this SEM (SE) image (Fig. 4) probably represent Al_2O_3 and TiO_2-rich regions, respectively. As TiO_2 has a lower mechanical strength than Al_2O_3, the TiO_2-rich lamellar zones will probably exhibit lower interlamellar strength, thereby lowering the coating toughness, as seen in Fig. 4.

On the other hand, the HVOF-sprayed hybrid coating (Fig. 5) exhibits a more homogenously mixed microstructure, which is probably the result of the intimate Al_2O_3 and TiO_2 particle mixing of the agglomerates (Fig. 2a). Based on the hypothesis proposed by Ahn et al. (Ref 2), this intimate Al_2O_3 and TiO_2 particle mixing would result in lowering the melting point of each agglomerate (TiO_2 addition to Al_2O_3) during thermal spraying, which would lower the viscosity of the particles. The lower viscosity would provide the splats improved wetting and interlamellar strength, thereby increasing coating toughness, as seen in Fig. 5.

It is important to point out that not all hybrid particles were fully molten during HVOF spraying. Figure 6 shows an SEM picture (SE) of the HVOF-sprayed hybrid

Table 3 Porosity and Vickers microhardness values of the Al_2O_3-13 wt.% TiO_2 coatings

Coating	P (%) (*n* = 10)	HV (300 gf) (*n* = 10)
APS Metco 130	1.9-4.7	970-1093
APS Nanox S2613S	2.6-4.4	776-1057
HVOF Amperit 744.0	2.2 ± 0.3	832 ± 41
HVOF Nanox S2613S	<1	808 ± 40

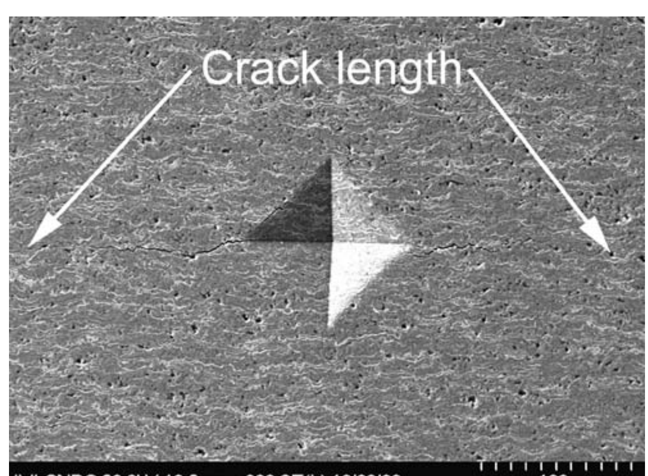

Fig. 4 Crack propagation under Vickers indentation for the HVOF-sprayed conventional (Amperit 744.0) coating

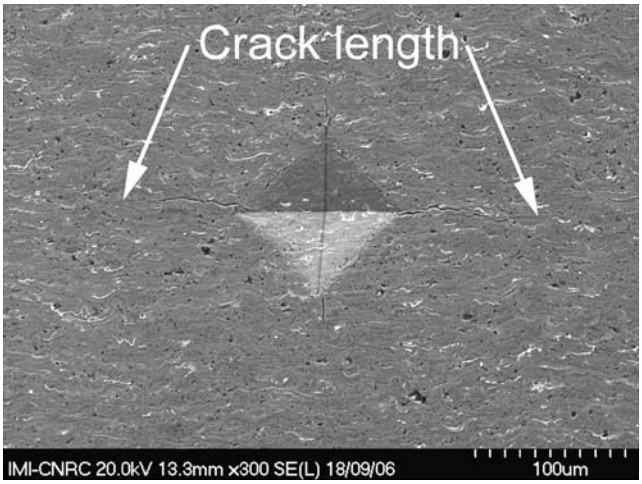

Fig. 5 Crack propagation under Vickers indentation for the HVOF-sprayed hybrid (Nanox S2613S) coating

(Nanox S2613S) coating of Fig. 5 taken at higher magnifications using different SEM conditions/parameters. It is possible to observe zones of finely dispersed material (similar to that found in HVOF-sprayed WC-Co coatings) spread throughout the coating microstructure (Fig. 6a), and Fig. 6b shows a high magnification view of one of these zones. By comparing these zones of finely dispersed material to the morphology of the Nanox S2613S hybrid powder (Fig. 2), it can be suggested that they probably correspond to semimolten hybrid particles that were embedded in the coating microstructure during HVOF spraying. It is also interesting to follow the path of the Vickers indentation cracks (such as that of Fig. 5) at higher magnifications (Fig. 6c). It was observed that the crack arrested after passing through a semimolten zone. It was also observed that the nonmolten nano and submicron particles diverted the crack, producing a more tortuous crack path helping to consume energy. This phenomenon is similar to that observed by Gell et al. for the same material (Ref 1).

It is important to point out that the original hybrid particles are porous (Fig. 2) as the result of the spray-drying process, however, the semimolten particles embedded in the coating microstructure are almost fully dense (Fig. 6b and c), i.e., the molten part of the feedstock fully or almost fully penetrated into the inner porous core of the particles during flight and/or at the impact with the substrate. Control of this phenomenon is very important in order to engineer coatings with high wear resistance levels, because porous zones embedded in the coating microstructure would lower its mechanical strength and integrity.

The percentage of semimolten hybrid particles embedded in the coating microstructure of the HVOF-sprayed coating was measured via image analysis, based on 10 SEM pictures taken using the same characteristics and magnification of Fig. 6a, and was found to be 52 ± 6%.

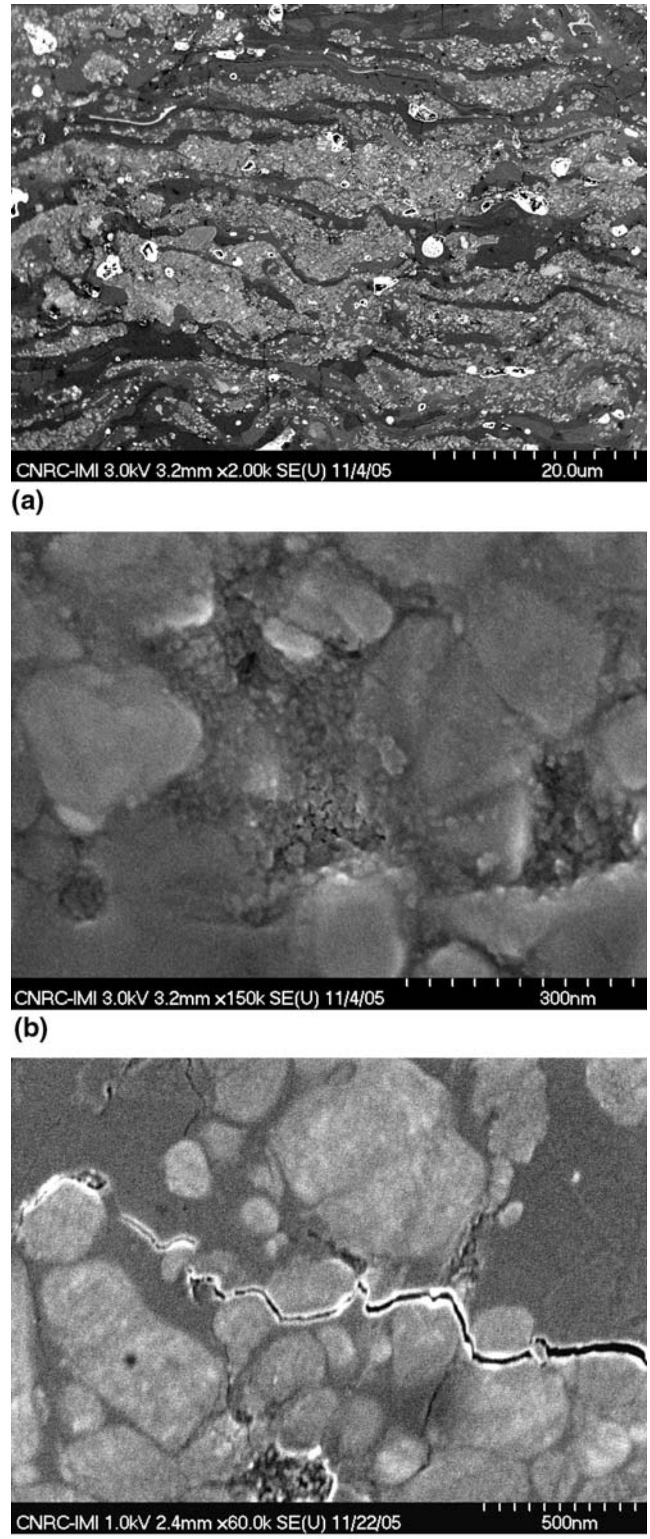

(c)

Fig. 6 (a) SEM picture of the HVOF-sprayed Nanox S2613S coating of Fig. 5 taken at higher magnifications—zones of finely dispersed material containing semimolten hybrid particles. (b) High magnification view of the dense finely dispersed zones. (c) Vickers indentation crack arrested after being diverted by passing through a semimolten hybrid particle (dense finely dispersed zone)

4. Conclusions

Three types of Al_2O_3-13 wt.% TiO_2 powders were employed in this study: one designated as ''hybrid,'' which was formed by agglomeration via the spray-drying of nanostructured and submicron particles (15-300 nm), and two conventional (blended and clad). The conclusions are the following:

- All four APS coatings produced from the conventional (clad) powder exhibited poorer abrasion wear resistance when compared to the three APS coatings produced from the hybrid powder. This result shows strong evidence of the superiority of the coatings made from the mixture of nanostructured and submicron particles concerning antiwear (abrasion) performance when compared to those made by conventional (clad) materials. When the optimized APS conventional (clad) coating is compared to the HVOF-sprayed hybrid coating, a reduction in volume loss of 87%, or an improvement of eight times in abrasion wear performance is observed for the HVOF-sprayed hybrid material.
- When the HVOF-sprayed hybrid coating is observed at high magnifications using SEM, it is possible to observe finely dispersed material zones ($52 \pm 6\%$ in cross-sectional area) spread throughout the coating microstructure, which correspond to semimolten hybrid powder particles embedded in the coating microstructure that are almost fully dense, i.e., the molten part of the feedstock fully or almost fully penetrated into the porous core of the particles during flight and/or at the impact with the substrate. Engineering dense finely dispersed zones is important to produce coatings with high wear resistance levels, because porous zones embedded in the coating microstructure would lower its mechanical strength and integrity.
- As observed by other authors (Ref 1, 2), the superior wear resistance of these ''nanostructured'' ceramic thermal spray coatings cannot be explained in terms of simple average hardness values. The factor (property) that seems to be most important for the superior antiwear performance of these coatings is the crack propagation resistance or toughness.
- It is hypothesized that two mechanisms are acting together for producing the enhanced toughness and superior wear resistance for the HVOF-sprayed hybrid coating. (i) The high degree of Al_2O_3 and TiO_2 mixing in each hybrid agglomerate probably lowers its melting point (addition of TiO_2 to Al_2O_3) producing a lowering of the particle viscosity (at least at the surface) and improving the interlamellar contact at impact during HVOF spraying. (ii) Cracks tend to lose their energy by being diverted when passing through the semimolten hybrid particles embedded in the coating microstructure.

References

1. M. Gell, E.H. Jordan, Y.H. Sohn, D. Goberman, L. Shaw, and T.D. Xiao, Development and Implementation of Plasma Sprayed Nanostructured Ceramic Coatings, *Surf. Coat. Technol.*, 2001, **146-147**, p 48-54
2. J. Ahn, B. Hwang, E.P. Song, S. Lee, and N.J. Kim, Correlation of Microstructure and Wear Resistance of Al_2O_3-TiO_2 Coatings Plasma Sprayed with Nanopowders, *Metall. Mater. Trans. A*, 2006, **37A**, p 1851-1861
3. R.S. Lima and B.R. Marple, From APS to HVOF Spraying of Conventional and Nanostructured Titania Feedstock Powders: a Study on the Enhancement of the Mechanical Properties, *Surf. Coat. Technol.*, 2000, **200**, p 3428-3437
4. G.R. Anstis, P. Chantikul, B.R. Lawn, and D.B. Marshall, A Critical Evaluation of Indentation Techniques for Measuring Fracture Toughness: I. Direct Crack Measurements, *J. Am. Ceram. Soc.*, 1981, **64**(9), p 1073-1082
5. Standard Test Method for Measuring Abrasion Using the Dry Sand/Rubber Wheel Apparatus, G65-00, *Annual Book of ASTM Standards*, ASTM 2000, p 1-12
6. R.S. Lima and B.R. Marple, Optimized HVOF Titania Coatings, *J. Therm. Spray Technol.*, 2003, **12**(3), p 360-368